A Novel Message Passing Based MIMO-OFDM Data Detector with a Progressive Parallel ICI Canceller

Chao-Wang Huang, Pang-An Ting, and Chia-Chi Huang

Abstract—A joint design of message passing MIMO data detector/decoder with progressive parallel inter-carrier interference canceller (PPIC) based on factor graph for OFDM-based wireless communication systems is proposed. By exchanging messages both in space domain and frequency domain, the proposed algorithm can suppress inter-antenna interferences and cancel inter-carrier interferences iteratively and progressively. With a proper designed message passing schedule and random interleaver, the short cycle problem is solved. Computer simulations show that the performance of the proposed message passing MIMO detector outperforms MMSE-SIC MIMO detector. The performances of PPIC, both in perfect channel estimation and imperfect channel estimation cases, are compared with the standard PIC architecture and the ICI self-canceller. The proposed PPIC is superior to PIC both in computational complexity and system architecture. The parallel structure of PPIC is similar to a systolic array. The proposed algorithm potentially leads to a very-high-speed detector/decoder. It is very suitable for VLSI implementation and it is a potential candidate for data detection/decoding in future high data rate, high mobility, wireless MIMO-OFDM communication systems.

Index Terms—MIMO-OFDM, data detection, ICI cancellation, message passing, factor graph, channel estimation error.

I. INTRODUCTION

WIDE band transmission with high spectral efficiency and high mobility is required for future mobile radio communications. MIMO technique with OFDM is one of the most promising techniques to achieve this goal. In a MIMO system, as data are transmitted/received through different antennas, many channel impairments need to be dealt with, such as multipath fading, AWGN noise, inter-antenna interference etc. To effectively deal with these channel impairments, many types of MIMO detectors such as MAP detector [1], sphere decoder [2], MMSE-SIC detector [1], [3], etc. have been proposed. For OFDM-based systems, the transmission bandwidth is divided into many narrow subchannels, which are transmitted in parallel. As a result, the symbol duration is increased and the intersymbol interference (ISI) caused by a multipath fading channel is alleviated. However, with longer symbol duration, channel's time variations lead to a loss of

subchannel orthogonality, known as inter-carrier interference (ICI). As delay spread increases, symbol duration should also increase in order to maintain a nearly flat channel in every frequency subband. Also due to high demand for bandwidth, there is a trend toward using higher frequency bands. As a result, the ICI effect becomes more severe as mobile speed, carrier frequency, and OFDM symbol duration increases. If it is not compensated, ICI will result in performance loss and an error floor that increases with Doppler frequency. In some circumstances, the ICI effect may degrade the BER performance significantly [4]–[6].

In recent years, ICI cancellation has received considerable attention. In [4], [7], [8], the performance degradation due to ICI is analyzed. It is shown that ICI can be modeled as an additive near-Gaussian random process that leads to an error floor which depends on the normalized Doppler frequency. In [9] and [10], the well-known ICI self-cancellation scheme is proposed. By appropriately mapping symbols to a group of subcarriers, the proposed algorithm in [9] makes OFDM transmissions less sensitive to the ICI at the cost of much lower bandwidth efficiency. In [11], it is shown that ICI power comes mainly from 12 neighboring subcarriers and based on this observation a low-complexity MMSE equalizer is proposed. Yet, as the MMSE equalizer still exhibits an error floor on BER, a low-complexity decision-feedback equalizer (DFE) is proposed in [11] to improve the performance. In [12], based on the piece-wise linear approximation on channel's time variations, two ICI mitigation methods are proposed for an OFDM system working in considerably large delay and Doppler spread environments, such as SFN and cellular networks. Furthermore, it is also shown in [12] how to estimate channel's time variations utilizing either the cyclic prefix or three consecutively transmitted symbols. In [13], an ICI reduction method is proposed based on a sphere decoding (SD) algorithm. By considering channel information, a new search strategy is developed to reduce the computational complexity of the SD algorithm. Because of the frequency diversity introduced by channel variations, performance can be improved by the proposed algorithm at higher Doppler frequencies.

In recent years, the message passing data detector/decoder catches the attention of many researchers. One appealing practical aspect of the message passing data detector/decoder is due to that it consists of many small, independent detection/decoding functions to deal with channel impairments.
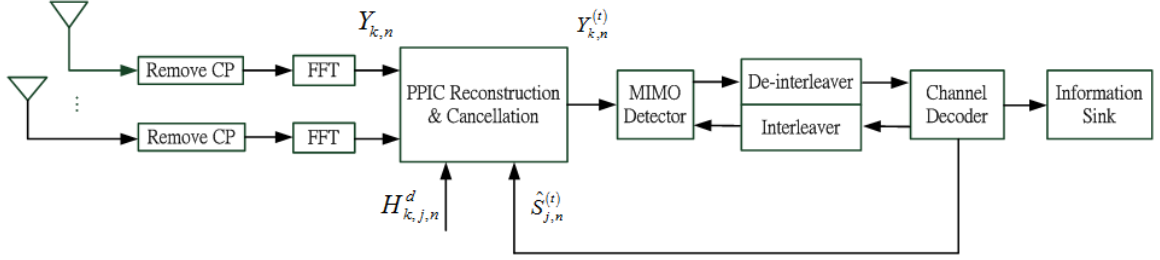
Fig. 1. Block diagram of the proposed message passing data detection/decoding and ICI cancellation scheme.

Hardware could be implemented according to these independent detectors/decoders and operated in parallel, and it potentially leads to a very-high-speed detector/decoder. This aspect is particularly important in data transmissions where data rate requirements are high, and processing delay must be low [14].

Digital implementations of message passing algorithm require real number arithmetic and are thus quite complex, and some researchers pointed out that message passing algorithms can be realized with simple analog transistor circuits. The attraction of such analog detector/decoder comes from that the iteration operation is actually the transient response. In other words, the detector/decoder is just an asynchronous electronic network that stabilizes in a state that corresponds to the transmitted symbols/codewords [15], [16]. More discussions and applications about factor graph and message passing algorithm can be found in [17], [18], [19].

Based on factor graph, a joint design of a message passing MIMO data detector/decoder with a progressive parallel inter-carrier interference canceller (PPIC) for OFDM-based wireless communication systems is proposed in this paper. The message type chosen in this work is log-likelihood ratio (LLR) of bit probabilities for the MIMO data detector/decoder and soft data symbols for the PPIC ICI canceller. The proposed algorithm detects the transmitted data iteratively, by jointly dealing with channel fading effects, AWGN noise and interferences in time domain, frequency domain and space domain. With the insertion of cyclic prefix, the time domain ISI can be avoided. With the message passing MIMO detector (denoted as MPD in the following sections), the space domain inter-antenna interference can be suppressed and with the aid of PPIC, the frequency domain ICI can be cancelled. Besides, the computational complexity of the proposed PPIC architecture is relatively lower than the standard PIC architecture. The system architecture is also simpler and more suitable for the VLSI implementation.

This paper is organized as follows: section II defines the system model of a wireless MIMO-OFDM communication system with ICI effects. The proposed message passing algorithm for LDPC-coded MIMO-OFDM systems is derived in section III. The Progressive PIC architecture is depicted in section IV. In section V, we discuss the schedule of message passing and the method to use interleaving to deal with the short-cycle problem. Section VI discusses the computational complexity and system architecture of the proposed algorithm. Simulation results of BER performance are given in section VII, and finally, in section VIII we conclude this paper.

II. SYSTEM MODEL

We assume perfect timing synchronization and both perfect and imperfect channel estimation in this paper. Consider an OFDM-based wireless MIMO communication system with N_t transmit and N_r receive antennas. The transmitted time domain signal can be represented by the following equation:

$$s_{j,i} = \frac{1}{N_c} \sum_{n=0}^{N_c-1} S_{j,n} e^{\frac{2\pi ni}{N_c}} \quad (1)$$

where $i = 0 \sim N_c - 1$, $j = 0 \sim N_t - 1$, N_c is the FFT size, $S_{j,n}$ is the symbol transmitted on the j_{th} antenna and n_{th} subcarrier and belonging to the constellation S with size $|S| = 2^m$, m is the modulation order, $s_{j,i}$ is the i_{th} sample of the time domain signal transmitted on the j_{th} antenna. The cyclic prefix vector can be represented as:

$$\vec{s}_{\text{CP},j}(i) = s_{j,N_c-N_G+i} \quad (2)$$

where $i = 0 \sim N_G - 1$, N_G is the length of guard interval. The i_{th} sample of the received time domain signal at the k_{th} antenna can be derived as:

$$y_{k,i} = \sum_{j=0}^{N_t-1} \sum_{l=0}^{N_G} h_{k,j,l}^{(i)} s_{j,\left((i-l)\right)_{N_c}} + z_{k,i} \quad (3)$$

where $i = 0 \sim N_c - 1$, $k = 0 \sim N_r - 1$, $h_{k,j,l}^{(i)}$ is the l_{th} channel tap gain between the j_{th} transmit antenna and k_{th} receive antenna, $\left((\cdot)\right)_{N_c}$ denotes a cyclic shift in the base of N_c and $z_{k,i}$ is a sample of AWGN noise with zero mean and variance σ_z^2. As shown in Fig. 1, after removing the cyclic prefix and FFT operations, the received frequency domain signal $Y_{k,n}$ can be formulated as:

$$
\begin{aligned}
Y_{k,n} &= \sum_{i=0}^{N_c-1} y_{k,i} e^{-j\frac{2\pi ni}{N_c}} \\
&= \sum_{j=0}^{N_t-1} H_{k,j,n}^0 S_{j,n} + \underbrace{\sum_{j=0}^{N_t-1} \sum_{d=1}^{N_c-1} H_{k,j,n}^d S_{j,\left((n-d)\right)_{N_c}}}_{\text{ICI term}} \\
&\quad + Z_{k,n}
\end{aligned}
\quad (4)
$$

where $n = 0 \sim N_c - 1$, d is the interfering subcarrier index. Define $F_l(n)$ as the FFT of the l_{th} channel tap with time variations:

$$F_l(n) = \sum_{i=0}^{N_c-1} h_{k,j,l}^{(i)} e^{-j\frac{2\pi ni}{N_c}} \quad (5)$$
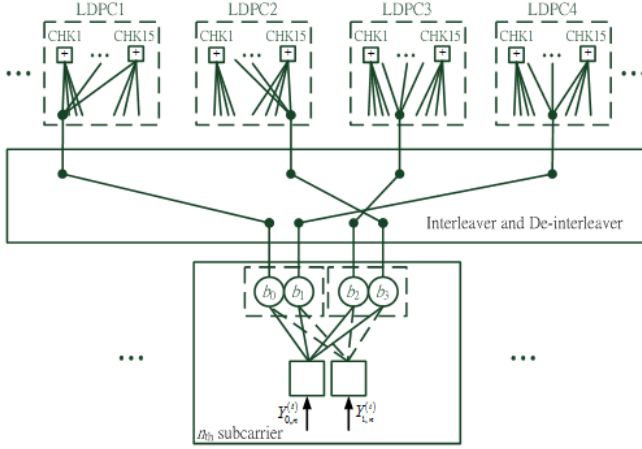
Fig. 2. Messages passing on factor graph for a 2×2 MIMO channel (QPSK case) and LDPC decoders.

where $l = 0\sim N_G - 1$, $n = 0\sim N_c - 1$. Then, the ICI channel coefficients in the frequency domain can be reformulated as:

$$H_{k,j,n}^d = \frac{1}{N_c}\sum_{l=0}^{N_G} F_l(d)e^{-j\frac{2\pi l(n-d)}{N_c}} \quad (6)$$

$$H_{k,j,n}^0 = \frac{1}{N_c}\sum_{l=0}^{N_G}\sum_{i=0}^{N_c-1} h_{k,j,l}^{(i)}e^{-j\frac{2\pi nl}{N_c}}$$

$$= \sum_{l=0}^{N_G} h_{k,j,l}^{\mathrm{ave}}e^{-j\frac{2\pi nl}{N_c}} \quad (7)$$

where $n, d = 0\sim N_c - 1$, $h_{k,j,l}^{\mathrm{ave}}$ is average of the l_{th} channel tap over the useful time duration of an OFDM symbol. Without loss of generality, in the following sections, only the n_{th} subcarrier of the MIMO-OFDM receiver is considered. Eq. (4) can be rewritten as:

$$\mathbf{Y}_n = \mathbf{H}_n^0\mathbf{S}_n + \sum_{d=1}^{N_c-1}\mathbf{H}_n^d\mathbf{S}_{\left((n-d)\right)_{N_c}} + \mathbf{Z}_n \quad (8)$$

where $\mathbf{Y}_n \equiv \left(Y_{0,n},...,Y_{(N_r-1),n}\right)^T$, $\mathbf{H}_n^0 \equiv \{H_{k,j,n}^0\}$ and $\mathbf{H}_n^d \equiv \{H_{k,j,n}^d\}$ are both $N_r\times N_t$ channel matrices, $\mathbf{S}_n \equiv \left(S_{0,n},...,S_{(N_t-1),n}\right)^T$, $\mathbf{Z}_n \equiv \left(Z_{0,n},...,Z_{(N_r-1),n}\right)^T$, $Z_{k,n}$ is an i.i.d. complex Gaussian noise with zero mean and variance σ_Z^2. Moreover, we define the input data of the n_{th} subcarrier as a binary $m\times N_t$-vector, $\mathbf{b}_n \equiv (\mathbf{b}_0,...,\mathbf{b}_{N_t-1})^T$, where $\mathbf{b}_j \equiv (b_{j,0},...,b_{j,m-1})$ and $b_{j,q}\in\{0,1\}$. The binary data vector $\mathbf{b}_n$ is mapped to the symbol vector $\mathbf{S}_n$.

III. MESSAGE PASSING ALGORITHM AND LDPC DECODER

A. Message Passing MIMO Detector (MPD)

Without consideration of PPIC in Fig. 1, to describe the function of an MPD for a MIMO-OFDM receiver, first, a factor graph for the 2×2 MIMO flat fading channel with QPSK modulation is constructed in Fig. 2. It is easily to extend Fig. 2 to general cases. The messages passed between variables are log-likelihood ratios of bit probabilities, $L_q = \ln[P(b_q = 0)/P(b_q = 1)]$. The transmit variable b_q,

defined as bit node on the factor graph, and the receive variable $Y_{k,n}$, defined as channel node on the factor graph, generate messages using sum-product rule [15], [20]. Let $\mathbf{b}$ represent bits $(b_0,...,b_{(mN_t-1)})^T$. The message generated by $Y_{k,n}$ and passed to b_q, called $L_{R(k\to q)}$ is

$$L_{R(k\to q)}$$
$$= \ln\frac{\sum_{\mathbf{b}:b_q=0}\{p(Y_{k,n}|\mathbf{b})\cdot\exp[\sum_{r=0,r\neq q,b_r=0}^{mN_t-1} L_{Q(r\to k)}]\}}{\sum_{\mathbf{b}:b_q=1}\{p(Y_{k,n}|\mathbf{b})\cdot\exp[\sum_{r=0,r\neq q,b_r=0}^{mN_t-1} L_{Q(r\to k)}]\}} \quad (9)$$

where $p(Y_{k,n}|\mathbf{b})$ is Gaussian distributed, and $L_{Q(r\to k)}$ is the extrinsic information.

Similarly, the term $L_{Q(r\to k)}$ in (9) is the message generated by b_r and passed to $Y_{k,n}$. This message is given by

$$L_{Q(r\to k)} = L_{a,r} + \sum_{p=0,p\neq k}^{N_r-1} L_{R(p\to r)} \quad (10)$$

where $L_{a,r} = \ln[P_a(b_r = 0)/P_a(b_r = 1)]$ and $P_a(b_r)$ denotes the a-priori probability of the transmitted bit b_r.

Finally, the decision variable, soft decision and hard decision for the r_{th} bit are given in (11), (12) and (13), respectively:

$$L_{Q,r} = L_{a,r} + \sum_{k=0}^{N_r-1} L_{R(k\to r)} \quad (11)$$

$$\tilde{b}_r = \tanh(0.5\cdot L_{Q,r}) \quad (12)$$

$$\hat{b}_r = \begin{cases}0, & L_{Q,r} \geq 0 \\ 1, & \text{otherwise}\end{cases} \quad (13)$$

B. LDPC Decoder

The message passing algorithm is also used to decode the LDPC code [21]. The messages L_U generated at the u_{th} code bit node and passed to the ν_{th} check nodes are calculated as:

$$L_{U(u\to\nu)} = \sum_{p=0}^{N_r-1} L_{R(p\to u)} \quad (14)$$

The messages L_V generated at the ν_{th} check node and passed to the u_{th} code bit nodes are calculated as:

$$L_{V(\nu\to u)}$$
$$= \prod_{\acute{u}=0,\acute{u}\neq u}^{d_c-1} sign\big(L_{U(\acute{u}\to\nu)}\big)\cdot\phi\bigg(\sum_{\acute{u}=0,\acute{u}\neq u}^{d_c-1}\phi\big(|L_{U(\acute{u}\to\nu)}|\big)\bigg) \quad (15)$$

where $\phi(x) = -\log[\tanh(x/2)] = \log[(e^x + 1)/(e^x - 1)]$ and d_c is the row weight of parity check matrix.

IV. PROGRESSIVE PIC ARCHITECTURE

As illustrated in Fig. 3, the PPIC architecture is modeled as a factor graph. The subcarrier nodes represented as blocks for ICI cancellation execute the function of interference reconstruction and cancellation. The message type is soft data symbol. The estimated soft data symbols are exchanged between adjacent subcarrier nodes and stored. At the 1_{st} iteration, the n_{th} subcarrier node receives and stores the soft symbols from the $(n+1)_{th}$ subcarrier node and the $(n-1)_{th}$ subcarrier node. These soft data symbols are used for ICI reconstruction and
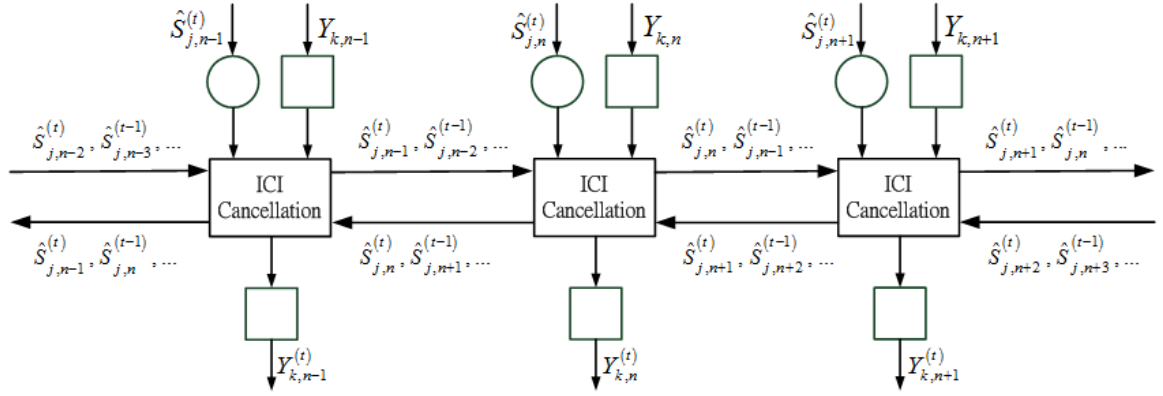
Fig. 3. Factor graph of the proposed PPIC architecture.

cancellation. So, the ICI from the $(n+1)_{th}$ subcarrier and the $(n-1)_{th}$ subcarrier are reconstructed and cancelled. At the 2_{nd} iteration, the n_{th} subcarrier node receives and stores the soft symbols, which are estimated at the 2_{nd} iteration, from the $(n+1)_{th}$ subcarrier node and the $(n-1)_{th}$ subcarrier node, and the soft symbols, which are stored at the 1_{st} iteration, from the $(n+1)_{th}$ subcarrier node and the $(n-1)_{th}$ subcarrier node. These stored data symbols are actually estimated by the $(n+2)_{th}$ subcarrier node and the $(n-2)_{th}$ subcarrier node at the 1_{st} iteration. So, the ICI from the $(n+1)_{th}$ subcarrier, $(n+2)_{th}$ subcarrier, $(n-1)_{th}$ subcarrier and $(n-2)_{th}$ subcarrier are reconstructed and cancelled. In this way, the ICI are reconstructed and cancelled iteratively and progressively from the received signal. At the 1st iteration, the two strongest interfering subcarriers are cancelled. At the 2_{nd} iteration, the two strongest and the two adjacent less strong interfering subcarriers are cancelled. At the i_{th} iteration, the ICI from $2i$ adjacent subcarriers are cancelled.

Stated more formally, at the 0_{th} iteration, the estimated soft data symbols for the j_{th} transmit antenna and the reconstructed ICI at the k_{th} receive antenna are initialized to $\mathbf{0}$:

$$\hat{\mathbf{S}}_j^{(0)} = \begin{bmatrix} \cdots & \hat{S}_{j,n-1}^{(0)} & \hat{S}_{j,n}^{(0)} & \hat{S}_{j,n+1}^{(0)} & \cdots \end{bmatrix} = \mathbf{0} \quad (16)$$

$$\hat{\mathbf{S}}_{\text{ICI},k}^{(0)}$$
$$= \begin{bmatrix} \cdots & \hat{S}_{\text{ICI},k,n-1}^{(0)} & \hat{S}_{\text{ICI},k,n}^{(0)} & \hat{S}_{\text{ICI},k,n+1}^{(0)} & \cdots \end{bmatrix} = \mathbf{0} \quad (17)$$

Hence, the ICI cancelled signals are exactly the same as the received signals:

$$\mathbf{Y}_k^{(0)} = \mathbf{Y}_k - \hat{\mathbf{S}}_{\text{ICI},k}^{(0)} = \mathbf{Y}_k \quad (18)$$

The results in (18) are fed forward to the MPD and LDPC decoder as described in section III to be further processed.

At the 1_{st} iteration, the estimated soft data symbols are fed back from the LDPC decoder. These soft data symbols are exchanged between adjacent subcarrier nodes and stored. Take the n_{th} subcarrier node for example, it receives and stores:

$$\hat{\mathbf{S}}_{j,n}^{(1)} = \begin{bmatrix} \hat{S}_{j,((n-1))_{N_c}}^{(1)} & \hat{S}_{j,((n+1))_{N_c}}^{(1)} \end{bmatrix} \quad (19)$$

According the results in (19), The ICI from the $(n+1)_{th}$ subcarrier and the $(n-1)_{th}$ subcarrier are reconstructed and

cancelled:

$$\hat{S}_{\text{ICI},k,n}^{(1)} = H_{k,j,n}^1 \cdot \hat{S}_{j,((n-1))_{N_c}}^{(1)} + H_{k,j,n}^{N_c-1} \cdot \hat{S}_{j,((n+1))_{N_c}}^{(1)} \quad (20)$$

$$\mathbf{Y}_k^{(1)} = \mathbf{Y}_k - \hat{\mathbf{S}}_{\text{ICI},k}^{(1)} \quad (21)$$

Afterwards, data are detected by the MPD and LDPC decoder.

At the 2_{nd} iteration, the processes in the 1_{st} iteration are repeated. The n_{th} subcarrier node receives and stores:

$$\hat{\mathbf{S}}_{j,n}^{(2)} = \begin{bmatrix} \hat{S}_{j,((n-2))_{N_c}}^{(1)} & \hat{S}_{j,((n-1))_{N_c}}^{(2)} \\ \hat{S}_{j,((n+1))_{N_c}}^{(2)} & \hat{S}_{j,((n+2))_{N_c}}^{(1)} \end{bmatrix} \quad (22)$$

So, the ICI from the $(n+1)_{th}$ subcarrier, $(n+2)_{th}$ subcarrier, $(n-1)_{th}$ subcarrier and $(n-2)_{th}$ subcarrier are reconstructed and cancelled:

$$\hat{S}_{\text{ICI},k,n}^{(2)} = H_{k,j,n}^1 \cdot \hat{S}_{j,((n-1))_{N_c}}^{(2)} + H_{k,j,n}^2 \cdot \hat{S}_{j,((n-2))_{N_c}}^{(1)}$$
$$+ H_{k,j,n}^{N_c-2} \cdot \hat{S}_{j,((n+2))_{N_c}}^{(1)} + H_{k,j,n}^{N_c-1} \cdot \hat{S}_{j,((n+1))_{N_c}}^{(2)} \quad (23)$$

$$\mathbf{Y}_k^{(2)} = \mathbf{Y}_k - \hat{\mathbf{S}}_{\text{ICI},k}^{(2)} \quad (24)$$

At the t_{th} iteration, the soft data symbols from the adjacent $2t$ subcarriers are received and stored by the n_{th} subcarrier node:

$$\hat{\mathbf{S}}_{j,n}^{(t)} = \begin{bmatrix} \hat{S}_{j,((n-t))_{N_c}}^{(1)} & \cdots & \hat{S}_{j,((n-2))_{N_c}}^{(t-1)} & \hat{S}_{j,((n-1))_{N_c}}^{(t)} \\ \hat{S}_{j,((n+1))_{N_c}}^{(t)} & \hat{S}_{j,((n+2))_{N_c}}^{(t-1)} & \cdots & \hat{S}_{j,((n+t))_{N_c}}^{(1)} \end{bmatrix} \quad (25)$$

The ICI from the adjacent $2t$ subcarriers can be reconstructed and cancelled:

$$\hat{S}_{\text{ICI},k,n}^{(t)} = H_{k,j,n}^1 \cdot \hat{S}_{j,((n-1))_{N_c}}^{(t)} + H_{k,j,n}^2 \cdot \hat{S}_{j,((n-2))_{N_c}}^{(t-1)}$$
$$+ \ldots + H_{k,j,n}^t \cdot \hat{S}_{j,((n-t))_{N_c}}^{(1)}$$
$$+ H_{k,j,n}^{N_c-t} \cdot \hat{S}_{j,((n+t))_{N_c}}^{(1)} + \ldots$$
$$+ H_{k,j,n}^{N_c-2} \cdot \hat{S}_{j,((n+2))_{N_c}}^{(t-1)} + H_{k,j,n}^{N_c-1} \cdot \hat{S}_{j,((n+1))_{N_c}}^{(t)} \quad (26)$$

$$\mathbf{Y}_k^{(t)} = \mathbf{Y}_k - \hat{\mathbf{S}}_{\text{ICI},k}^{(t)} \quad (27)$$

Further more, each column of the channel matrix $\mathbf{H}_{k,j}$, as shown in (28), is calculated only when it is needed.

In the 0_{th} iteration, $\mathbf{H}_{k,j}^0 = \begin{bmatrix} H_{k,j,0}^0 & \cdots & H_{k,j,N_c-1}^0 \end{bmatrix}^T$ needs to be calculated. In the 1_{st} iteration,

$$\mathbf{H}_{k,j} = \begin{bmatrix} H_{k,j,0}^0 & H_{k,j,0}^1 & H_{k,j,0}^2 & \cdots & H_{k,j,0}^{N_c-2} & H_{k,j,0}^{N_c-1} \\ H_{k,j,1}^0 & H_{k,j,1}^1 & H_{k,j,1}^2 & \cdots & H_{k,j,1}^{N_c-2} & H_{k,j,1}^{N_c-1} \\ \vdots & \vdots & \vdots & \ddots & \vdots & \vdots \\ H_{k,j,N_c-2}^0 & H_{k,j,N_c-2}^1 & H_{k,j,N_c-2}^2 & \cdots & H_{k,j,N_c-2}^{N_c-2} & H_{k,j,N_c-2}^{N_c-1} \\ H_{k,j,N_c-1}^0 & H_{k,j,N_c-1}^1 & H_{k,j,N_c-1}^2 & \cdots & H_{k,j,N_c-1}^{N_c-2} & H_{k,j,N_c-1}^{N_c-1} \end{bmatrix} \tag{28}$$

$\mathbf{H}_{k,j}^1 = \begin{bmatrix} H_{k,j,0}^1 & \cdots & H_{k,j,N_c-1}^1 \end{bmatrix}^T$ and $\mathbf{H}_{k,j}^{N_c-1} = \begin{bmatrix} H_{k,j,0}^{N_c-1} & \cdots & H_{k,j,N_c-1}^{N_c-1} \end{bmatrix}^T$ need to be calculated. In the 2_{nd} iteration, $\mathbf{H}_{k,j}^2 = \begin{bmatrix} H_{k,j,0}^2 & \cdots & H_{k,j,N_c-1}^2 \end{bmatrix}^T$ and $\mathbf{H}_{k,j}^{N_c-2} = \begin{bmatrix} H_{k,j,0}^{N_c-2} & \cdots & H_{k,j,N_c-1}^{N_c-2} \end{bmatrix}^T$ need to be calculated and so forth. Two more columns of the matrix are calculated at every iteration and two more interfering subcarriers are cancelled at each iteration. At last, the ICI cleaned signal $Y_{k,n}^{(t)}$ is fed forward to the MPD, as shown in Fig. 1. The proposed algorithm can suppress multiple-antenna interferences and cancel inter-carrier interferences iteratively and progressively until a stopping criterion is satisfied. The estimated soft data symbols are calculated using (29) for QPSK or (30) for 16-QAM:

$$\hat{S}_{j,n}^{(t)} = \frac{1}{\sqrt{2}} \cdot \tilde{b}_{mj,n} + j\frac{1}{\sqrt{2}} \cdot \tilde{b}_{mj+1,n} \tag{29}$$

$$\hat{S}_{j,n}^{(t)} = -\frac{1}{\sqrt{10}} \cdot \tilde{b}_{mj,n} \cdot \left(2 + \tilde{b}_{mj+2,n}\right)$$
$$-j\frac{1}{\sqrt{10}} \cdot \tilde{b}_{mj+1,n} \cdot \left(2 + \tilde{b}_{mj+3,n}\right) \tag{30}$$

where the soft bit information are obtained from (12).

V. MESSAGE PASSING SCHEDULE AND INTERLEAVING

With message passing algorithms, a cycle-free factor graph in general guarantees an exact solution. However, when a factor graph has many length-four cycles, it is likely that the message passing algorithm operated on the graph will not produce an exact solution. In such a case, the BER performance tends to improve very slowly with the number of iterations, even at very high SNR [14], [17]. More discussions about the short cycle problem of message passing algorithm can be found in [22]. As shown in Fig. 1, the received frequency domain signals are fed forward to PPIC ICI canceller first. After the ICI cancellation, the signal are fed forward to MPD and then to LDPC decoder. As illustrated in Fig. 2 and Fig. 3, the factor graph of the PPIC canceller has no cycle, however, that of the MIMO detector and LDPC decoder has a lot of short cycles. This problem needs to be dealt with or the performance of the proposed algorithm will be degraded. In order to deal with the short cycle problem of a factor graph, two algorithms are proposed in [23] to reduce the absolute value of the outgoing log-likelihood ratio messages at variable nodes by using multiplicative factor and an additive factor, respectively. In this paper, LDPC code and random interleaver with proper message passing schedule are exploited to solve this problem.

In order to improve the system performance, Gallager code [24] is used in the frequency domain. Due to the short codeword length of Gallager code, the encoder and decoder are relatively simpler than a long-length LDPC code. With the joint design of Gallager code, however, the cycle condition becomes worse since the cycles not only exist in the space domain but also in the frequency domain. To solve this problem, a properly designed frequency domain random interleaver has to be used with LDPC code. The design criterion is that the coded bits in the same codeword have to be sent to different subcarriers after interleaving. In other words, at the receiver, the detected bit messages in a subcarrier are de-interleaved to different channel decoders, as illustrated in Fig. 2. Then, with a properly designed message passing schedule, the bit information is passed both in the space domain and the frequency domain. In this way, the short cycle problem is solved.

In summary, seven steps are included in the message passing schedule. 1. The estimated soft data symbols, which are fed back from LDPC decoder, are exchanged between adjacent subcarrier nodes and stored as shown in Fig. 3. 2. The ICI are reconstructed and cancelled from the received signals and then the ICI cancelled signals are fed forward to the MPD as shown in Fig. 1. As shown in Fig. 2, 3. After the bit messages $L_{R(k\to q)}$ are generated by using (9) by the channel nodes at every subcarrier, these messages are passed to bit nodes. 4. After the messages $L_{U(q\to\nu)}$ are generated by using (14) and de-interleaved, these messages are passed to code bit nodes and then passed to check nodes of every LDPC decoder. Messages generated in a subcarrier are sent to different LDPC decoders. 5. The messages $L_{V(\nu\to u)}$ generated by check nodes using (15) are passed to code bit nodes and then interleaved. The messages generated by every coded bit node of the same LDPC decoder are sent to bit nodes which belong to different subcarriers. 6. The messages $L_{Q(u\to p)}$ are generated by bit nodes using (10) and then, passed to channel nodes. 7. Finally, the soft decision of data bits and data symbols are obtained by using (12) and (29) and then fed back to the PPIC canceller as depicted in Fig. 1. By iterative detection, decoding and progressive ICI cancellation, the system performance can be jointly optimized.

VI. COMPLEXITY

The order of computational complexity of the proposed MPD is $\mathcal{O}\{N_c N_r 2^{mN_t}\}$. It is feasible when m, N_t, N_r and N_c are small. Yet, the log-domain algorithm transforms multiplications of probabilities into additions of LLRs, which reduces the computational complexity significantly. Nevertheless, the computational complexity can be further reduced. In a fading
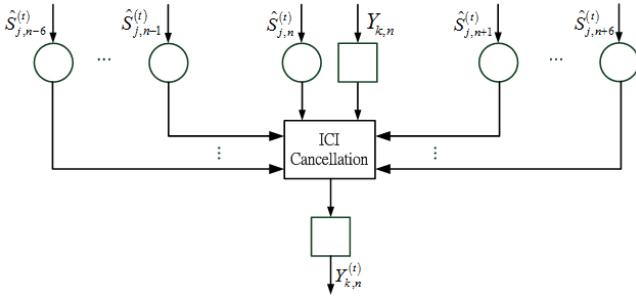
Fig. 4.   An architecture of PIC ICI canceller.

channel, the channel gains vary with time; hence the value of the information passed along the edges of the factor graph also varies with time. By exploiting this phenomenon, the edges with low importance, which is corresponding to the deep-faded channel gain, can be ignored. Since the number of edges of the factor graph is reduced, the computational complexity of the proposed algorithm is also reduced. There are several criteria which can be applied to determine which edges should be ignored. For example, the edges corresponding to the channel gains which are 5 dB smaller then the average channel gain are ignored or the four edges corresponding to the four smallest channel gains are ignored. In the former case, the number of ignored edges varies with time, however, in the latter case, it is fixed.

For PPIC ICI canceller, The computational complexity is in the order of $\mathcal{O}\{N_c(N_r N_t + m N_t)\}$. Moreover, due to the progressive architecture of PPIC, the computational complexity of each iteration is different. As the iterative process goes, the computational complexity of each iteration of PPIC monotonically increases. This is different from the standard PIC architecture which has constant computational complexity in each iteration. Overall, the computation complexity of PPIC is lower than PIC. The low complexity of PPIC makes it attractive for realizing the ICI cancellation of the future OFDM-based, high data rate, high mobility, wireless MIMO communication systems.

Moreover, the system architecture of PPIC is much simpler than PIC [25]. As shown in Fig. 3, the architecture of PPIC is similar to a systolic array [26]. Each subcarrier node is only connected to the adjacent two subcarrier nodes and exchanges messages with them. Nevertheless, as shown in Fig. 4, if the adjacent twelve interfering subcarriers are intended to be cancelled, each subcarrier node of the PIC architecture is connected to the adjacent twelve subcarrier nodes, and receives messages from them. This complicates the system architecture design of the standard PIC ICI canceller. Based on factor graph, the parallel structure of the proposed message passing MIMO data detector/decoder with PPIC ICI canceller is very suitable for VLSI implementation, especially for high speed analog detector/decoder where the iteration operation is actually a transient response and the high demand of computational complexity can be released.

VII. SIMULATION RESULTS OF BER PERFORMANCE

The BER performance of the proposed message passing algorithm on factor graph for data detection/decoding and ICI
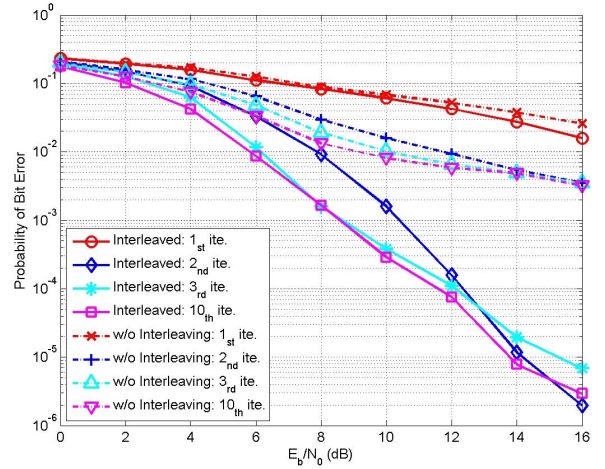

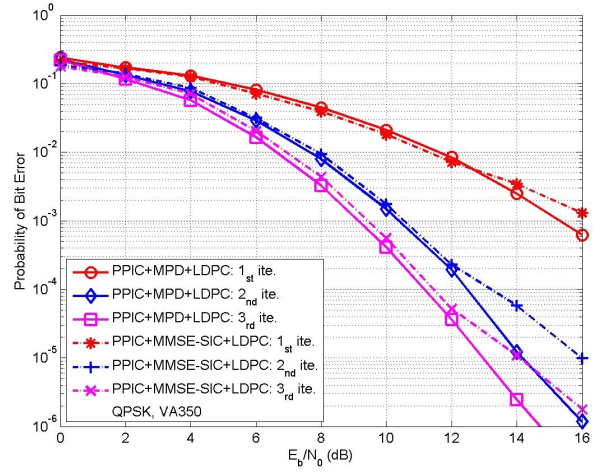Fig. 5.   With interleaving vs. without interleaving.

Fig. 6.   Performance comparison of message passing MIMO detector and MMSE-SIC MIMO detector.

cancellation in bit-interleaved LDPC-coded MIMO-OFDM systems are simulated with $N_t = N_r = 2$ and QPSK modulation. Gallager code with codeword length 20 is used. The dimension of the parity check matrix of Gallager code is 15×20 with row weight $d_c = 4$ and column weight $d_v = 3$ [27]. The FFT size of OFDM modulator is 1024. An S-random interleaver [28] of length 8192, $S = 64$ is used after the LDPC encoding. The multipath channel model is the ITU vehicular A channel. The fading channel model used is the Jakes' model [29]. In the case of imperfect channel estimation, two different models are used to model the variance of channel estimation error: a) σ_E^2 is independent of the SNR. b) σ_E^2 is a decreasing function of SNR [30], [31]. The carrier frequency is 2.5 GHz, bandwidth is 10 MHz, sampling frequency is 11.2 MHz, subcarrier spacing is 10.93 kHz, useful OFDM symbol duration is 91.43 μs and the length of cyclic prefix is 1/8 [32]. The vehicular speeds are 350 km/h which are corresponding to maximum Doppler frequency 810 Hz and normalized Doppler frequency 0.07.

The performances of the proposed algorithm with inter-

TABLE I
COMPARISONS OF PPIC, PIC AND ICI SELF-CANCELLER

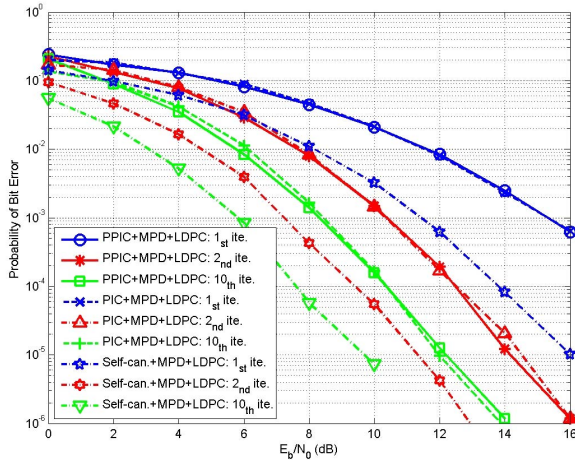|	PPIC ICI Canceller	PIC ICI Canceller	ICI Self-canceller
Performance	The same as PIC	The same as PPIC	2∼3 dB better
Complexity	Moderate	Most complicated	Easiest
Architecture	Simple	Complicated	Simple
Spectrum Efficiency	100%	100%	50%

Fig. 7.   Performance comparison of PPIC ICI canceller, PIC ICI canceller and ICI Self-canceller.
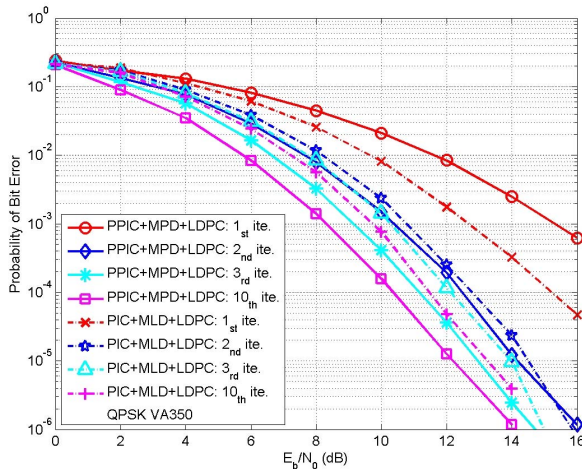

Fig. 8.   PPIC+MPD+LDPC vs. PIC+MLD+LDPC.

leaving and without interleaving are compared in Fig. 5. It is obvious that the system performance is not improved with LDPC code without interleaving. This is because the cycle condition of the coded case is more serious than the uncoded case as the cycles not only exist in the space domain but also in the frequency domain. In order to optimize the system performance and deal with the short cycle problem, an S-random interleaver is used after the LDPC encoding. The performance of the proposed algorithm is improved significantly and the length-four cycle problem is solved. With the message passing schedule of section V, the performance

comparison of MPD and MMSE-SIC is shown in Fig. 6. When the E_b/N_0 is smaller than 12 dB, the performance of MPD and MMSE-SIC are almost the same. However, when the E_b/N_0 is larger than 12 dB, MPD outperforms MMSE-SIC. When the BER is 10^{-5}, the performance of MPD is 1∼2 dB better than MMSE-SIC at the 2_{nd} and 3_{rd} iteration. MMSE-SIC still has an error floor when the E_b/N_0 is larger than 12 dB. In Fig. 7, the performance of PPIC ICI canceller is compared with a standard PIC ICI canceller, which cancels 12 adjacent interfering subcarriers at every iteration, and an ICI Self-canceller. The performances of PPIC ICI canceller and PIC ICI canceller are almost the same. Before the 6_{th} iteration, although the PIC ICI canceller cancels more interfering subcarriers than PPIC ICI canceller, it does not outperform PPIC ICI canceller. The reason is that if the estimated data symbols are not accurate enough, the ICI may be increased instead of reduced after cancellation. For the ICI self-cancellation, a data pair $(\mathcal{S}, -\mathcal{S})$ is modulated onto two adjacent subcarriers where $\mathcal{S}$ is a complex data symbol. The ICI generated within a group can be self-cancelled on each other. The performance of ICI self-canceller is 2∼3 dB better than PPIC ICI canceller at the price of half bandwidth efficiency. Comparisons of PIC ICI canceller, standard PIC ICI canceller and ICI Self-canceller are summarized in Table I. In Fig. 8, the performance of MPD is compared with maximum likelihood MIMO detector (denoted as MLD). It is obvious that PIC+MLD+LDPC performs better in the 1_{st} iteration. However, after the 2_{nd} iteration, PPIC+MPD+LDPC performs better. This is because MPD can exploit the fed back $a\text{-}priori$ information to approach the maximum $a\text{-}posteriori$ (MAP) solution but MLD only can approach the ML solution. The performance of the proposed algorithm with imperfect channel estimation is shown in Fig. 9. The variances of channel estimation error are 0.01, 0.1 and $0.03 + 0.8/SNR$ respectively, similar to those used in [30] and [31]. In each iteration, it is assumed that the channel coefficients are re-estimated and the variances of channel estimation error are assumed to be reduced 3 dB. When $\sigma_E^2 = 0.01$, the performance has almost no degradation. Yet, if $\sigma_E^2 = 0.03 + 0.8/SNR$, the performance may degrade 4 dB when BER is 10^{-2} in the 1_{st} iteration. In the 10_{th} iteration, however, the performances are almost the same since σ_E^2 is reduced 3 dB in each iteration. The performances of PPIC and PIC in the case of imperfect channel estimation are compared in Fig. 10. Their performances have almost no difference as observed from Fig. 10.

VIII. CONCLUSIONS

Based on factor graph, a joint design of message passing MIMO data detector/decoder with PPIC ICI canceller for
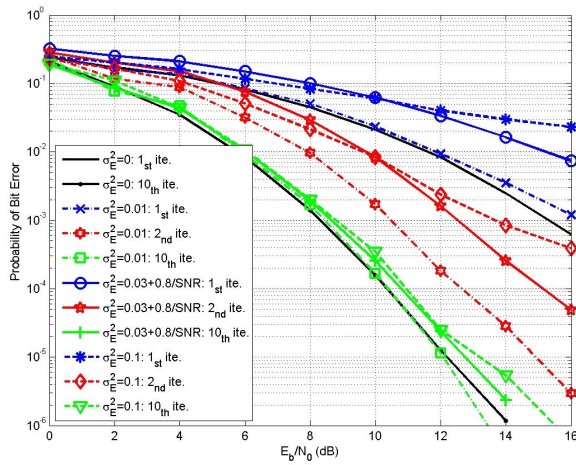
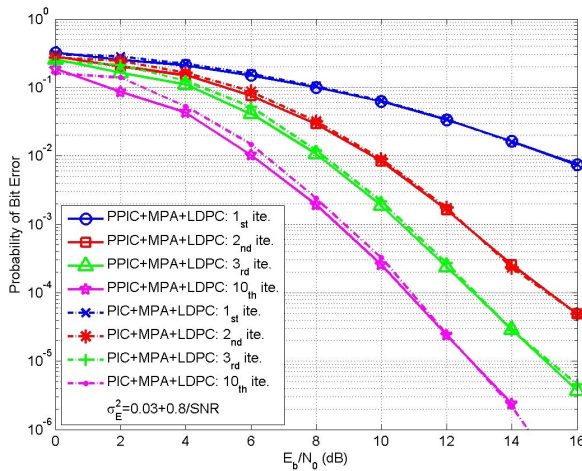Fig. 9. Imperfect channel estimation: PPIC+MPD+LDPC.

Fig. 10. Imperfect channel estimation: PPIC+MPD+LDPC vs. PIC+MPD+LDPC.

OFDM-based wireless communication systems is proposed. The proposed algorithm can suppress inter-antenna interferences in space domain and cancel inter-carrier interferences in frequency domain iteratively and progressively. With a proper designed message passing schedule and random interleaver, the short cycle problem is solved. Computer simulations show that the performance of MPD outperforms MMSE-SIC when the E_b/N_0 is larger than 12 dB. The performances of PPIC ICI canceller and standard PIC ICI canceller are almost the same both in perfect channel estimation and imperfect channel estimation cases; however, the computational complexity of PPIC is relatively lower. The system architecture of PPIC is also simpler than PIC. The performance of ICI self-canceller is 2~3 dB better than PPIC ICI canceller but at the price of half bandwidth efficiency. The parallel structure of the proposed message passing MIMO data detector/decoder with PPIC ICI canceller is very suitable for VLSI implementation. It is a potential candidate for data detection/decoding in future high data rate, high mobility, wireless MIMO-OFDM communication systems.

REFERENCES

[1] E. Biglieri, A. Nordio, and G. Taricco, "EXIT-chart analysis of iterative MIMO interfaces," *ISITA2004*, Oct. 2004.

[2] A. D. Kora, A. Saemi, J. P. Cances, and V. Meghdadi, "New list sphere decoding (LSD) and iterative synchronization algorithms for MIMO-OFDM detection with LDPC FEC," *IEEE Trans. Veh. Technol.*, vol. 57, no. 6, pp. 3510-3524, Nov. 2008.

[3] L. Ben, G. Yue, and X. Wang, "Performance analysis and design optimization of LDPC-coded MIMO OFDM systems," *IEEE Trans. Signal Process.*, vol. 52, no. 2, pp. 348-361, Feb. 2004.

[4] M. Russell and G. L. Stuber, "Interchannel interference analysis of OFDM in a mobile environment," in *Proc. IEEE VTC*, pp. 820-824, vol. 2, July 1995.

[5] K. Sathananthan and C. Tellambura, "Probability of error calculation of OFDM systems with frequency offset," *IEEE Trans. Commun.*, vol. 49, no. 11, pp. 1884-1888, Nov. 2001.

[6] T. Pollet, M. Van Bladel, and M. Moeneclaey, "BER sensitivity of OFDM systems to carrier frequency offset and Wiener phase noise," *IEEE Trans. Commun.*, vol. 43, no. 234, pp. 191-193, Feb.-Mar.-Apr. 1995.

[7] P. Robertson and S. Kaiser, "The effects of Doppler spreads in OFDM(A) mobile radio systems," in *Proc. IEEE VTC Fall*, vol. 1, pp. 329-333, Sep. 1999.

[8] Y. Li and L. J. Cimini, Jr., "Bounds on the interchannel interference of OFDM in time-varying impairments," *IEEE Trans. Commun.*, vol. 49, no. 3, pp. 401-404, Mar. 2001.

[9] Y. Zhao and S. G. Haggman, "Intercarrier interference self-cancellation scheme for OFDM mobile communication systems," *IEEE Trans. Commun.*, vol. 49, no. 7, pp. 1185-1191, July 2001.

[10] Y. Wang, S. Zhu. and Y. Li, "A method to improve the bandwidth efficiency of self ICI cancellation in OFDM systems," in *Proc. International Conf. Signal Process.*, vol. 2, pp. 1633-1636, 2002.

[11] X. Cai and G. B. Giannakis, "Bounding performance and suppressing intercarrier interference in wireless mobile OFDM," *IEEE Trans. Commun.*, vol. 51, no. 12, pp. 2047-2056, Dec. 2003.

[12] Y. Mostofi and D. C. Cox, "ICI mitigation for pilot-aided OFDM mobile systems," *IEEE Trans. Wireless Commun.*, vol. 4, no. 2, pp. 765-774, Mar. 2005.

[13] Y. J. Kou, W. S. Lu, and A. Antoniou, "Application of sphere decoding in intercarrier-interference reduction for OFDM systems," in *Proc. IEEE Pacific Rim Conf. Commun., Comput. Signal Process.*, pp. 360-363, Aug. 2005.

[14] B. M. Kurkoski, P. H. Siegel, and J. K. Wolf, "Joint message-passing decoding of LDPC codes and partial-response channels," *IEEE Trans. Inf. Theory*, vol. 48, no. 6, pp. 1410-1422, June 2002.

[15] H. A. Loeliger, "An introduction to factor graphs," *IEEE Signal Process. Mag.*, vol. 21, no. 1, pp. 28-41, Jan. 2004.

[16] H. A. Loeliger, F. Lustenberger, M. Helfenstein, and F. Tarkoy, "Probability propagation and decoding in analog VLSI," *IEEE Trans. Inf. Theory*, vol. 47, no. 2, pp. 837-843, Feb. 2001.

[17] M. N. Kaynak, T. M. Duman, and E. M. Kurtas, "Belief propagation over frequency selective fading channels," in *Proc. IEEE VTC-Fall*, vol. 2, pp. 1367-1371, 2004.

[18] B. Lu, G. Yue, X. Wang, and M. Madihian, "Factor-graph-based soft self-iterative equalizer for multipath channels," *EURASIP J. Wireless Commun. Netw.*, vol. 2005, no. 2, pp. 187-196, 2005.

[19] T. Wo and P. A. Hoeher, "A simple iterative Gaussian detector for severely delay-spread MIMO channels," *IEEE Int. Conf. Commun.*, June 2007.

[20] F. R. Kschischang, B. J. Frey, and H. A. Loeliger, "Factor graphs and the sum-product algorithm," *IEEE Trans. Inf. Theory*, vol. 47, no. 2, pp. 498-519, Feb. 2001.

[21] S. Papaharalabos, P. Sweeney, B. G. Evans, G. Albertazzi, A. Vanelli-Coralli, and G. E. Corazza, "Performance evaluation of a modified sum-product decoding algorithm for LDPC codes," in *Proc. 2nd International Symp. Wireless Commun. Syst.*, pp. 800-804, 2005.

[22] B. J. Frey and D. J. C. Mackay, "A revolution: belief propagation in graphs with cycles," in *Advances in Neural Information Processing Systems 10*. MIT Press, 1998.

[23] M. R. Yazdani, S. Hemati, and A. H. Banihashemi, "Improving belief propagation on graphs with cycles," *IEEE Commun. Lett.*, vol. 8, no. 1, pp. 57-59, 2004.

[24] R. Gallager, "Low-density parity-check codes," *IRE Trans. Inf. Theory*, pp. 21-28, Jan. 1962.

[25] D. Divsalar and M. K. Simon, "Improved CDMA performance using parallel interference cancellation," in *Proc. IEEE MILCOM '94*, vol. 3, pp. 911-917.

[26] S. Y. Kung, *VLSI Array Processors*. Prentice Hall, 1988.

[27] H. Robert and M. Zaragoza, *The Art of Error Correcting Coding*, 2nd edition. John Wiley & Sons, 2006.

[28] L. Dinoi and S. Benedetto, "Design of fast-prunable S-random interleavers," *IEEE Trans. Wireless Commun.*, vol. 4, no. 5, pp. 2540-2548, Sep. 2005.

[29] W. C. Jakes, *Microwave Mobile Communications*, 2nd edition. IEEE Press, 1993.

[30] T. Yoo and A. Goldsmith, "Capacity and power allocation for fading MIMO channels with channel estimation error," *IEEE Trans. Inf. Theory*, vol. 52, pp. 2203-2214, 2006.

[31] S. Han, S. Ahn, E. Oh, and D. Hong, "Effect of channel-estimation error on BER performance in cooperative transmission," *IEEE Trans. Veh. Technol.*, vol. 58, no. 4, pp. 2083-2088, 2009.

[32] IEEE 802.16m-08/004r5 EMD Document, 2009-01-15. Available: http://grouper.ieee.org/groups/802/16/tgm/docs/80216m-08_004r5.zip

Chao-Wang Huang received the B.S. and M.S. degrees in Electronics Engineering from National Chiao Tung University, Hsinchu, Taiwan in 1996 and 1998, respectively. Since 2007, he joined the Industrial Technology Research Institute (ITRI), Hsinchu, Taiwan, as an engineer. He is now studying for the Ph.D. program in National Chiao Tung University.

Pang-An Ting received the B.S. degree from the National Taiwan University of Science and Technology, Taipei, Taiwan, in 1991, and received the MS and Ph.D. degrees in electrical engineering, National Tsing Hua University, Taiwan, in 1994 and 2006, respectively. Since 1995, he joined the Industrial Technology Research Institute (ITRI), Hsinchu, Taiwan, as an engineer, senior engineer and project leaders for SoC designs of WiFi, WCDMA and WiMAX. His research interests are in the areas of wireless communications, statistic signal processing, and VLSI signal processing.

Chia-Chi Huang was born in Taiwan, R.O.C. He received the B.S. degree in electrical engineering from National Taiwan University in 1977 and the M.S. and Ph.D. degrees in electrical engineering from the University of California, Berkeley, in 1980 and 1984, respectively. From 1984 to 1988, he was an RF and Communication System Engineer with the Corporate Research and Development Center, the General Electric Company, in Schenectady, NY, where he worked on mobile radio communication system design. From 1989 to 1992, he was with the IBM T.J. Watson Research Center, in Yorktown Heights, NY, as a Research Staff Member, working on indoor radio communication system design. Since 1992, he has been with the National Chiao Tung University in Hsinchu, Taiwan, as a faculty member. Currently, he is a professor in the Department of Electrical Engineering.